International Journal of Geo-Information

MDPI

Article

Geological Hazard Assessment of Secondary Collapses Due to Volcanic Earthquakes on Changbai Mountain in China

Zengkai Pan [1], Qiuling Lang [2,*], Yichen Zhang [2], Jiquan Zhang [3], Chenglong Yu [2] and Chenyang Wu [1]

[1] School of Survey and Surveying Engineering, Changchun Institute of Technology, Changchun 130012, China
[2] School of Jilin Emergency Management, Changchun Institute of Technology, Changchun 130012, China
[3] School of Environment, Northeast Normal University, Changchun 130117, China
* Correspondence: langqiuling@tom.com; Tel.: +86-15104417089

Abstract: In recent years, the volcanic activity of Changbai Mountain has been accompanied by several earthquakes, and the frequent human engineering activities have led to a gradual increase in the number of collapses in the region, which severely impacts residents' lives and property safety. In northeastern China, the Changbai Mountain area in the southeastern Jilin Province is a typical mountain environment. This paper selects 12 evaluation indicators to build a hazard assessment system, including slope, aspect, elevation, curvature, lithology, NDVI, land use type, distance from the fault, the river from the road, volcanic earthquake, and annual average precipitation. Using emotional weight (G1 method) and objective weight (WOE-CV method), the hazard due to collapses in the study area is evaluated too. Among them, the transcendence probability of volcanic earthquakes greater than VI degree represents the relationship between Changbai Mountain volcanic earthquakes and the assessment of geological collapse hazard. The results show that high- and very high-hazard areas are mainly distributed in densely populated areas and national and provincial trunk lines, with apparent spatial agglomeration characteristics. The low-hazard area, medium-hazard area, high-hazard area and very high-hazard area accounted for 19.33%, 44.19%, 33.85% and 2.63% of the total area of the study area, respectively. By comparing the previous geological hazard survey reports in the area with the collapse hazard zoning map in this paper, 87.72% of the known collapse hazard areas are distributed within high and very high hazard zones, indicating that the conclusions of the article are more accurate and in line with the actual situation. Results from collapse-related hazards can provide relevant guidance for preventing and controlling geological risks posed by volcanic earthquakes affecting Changbai Mountain.

Keywords: collapse; Changbai Mountain; combination weight; hazard assessment; volcanic earthquake

check for updates

Citation: Pan, Z.; Lang, Q.; Zhang, Y.; Zhang, J.; Yu, C.; Wu, C. Geological Hazard Assessment of Secondary Collapses Due to Volcanic Earthquakes on Changbai Mountain in China. *ISPRS Int. J. Geo-Inf.* **2023**, *12*, 307. https://doi.org/10.3390/ijgi12080307

Academic Editors: Wolfgang Kainz and Godwin Yeboah

Received: 10 May 2023
Revised: 14 July 2023
Accepted: 19 July 2023
Published: 28 July 2023

Copyright: © 2023 by the authors. Licensee MDPI, Basel, Switzerland. This article is an open access article distributed under the terms and conditions of the Creative Commons Attribution (CC BY) license (https://creativecommons.org/licenses/by/4.0/).

1. Introduction

In the past few years, with the continuous development of cities and the increasing number of human activities, the disruption of ecological environments has led to the increasing frequency of geological related hazards, and the economic losses caused by hazards are also increasing [1,2]. As the world's second largest economy, China's economic growth has always been in the forefront of the world. How to reduce the losses caused by disasters while maintaining economic development is an important part of disaster prevention and reduction, Therefore, it is of great significance to carry out hazard assessments concerning geological hazards [3].

Changbai Mountain is a famous tourist attraction and an important part of the region's economic development. With a nearby resident population in the tens of millions, in the event of eruptive activity from the Changbai Mountain Volcano, the resulting secondary geological hazards could cause huge economic losses and human casualties. From 2002 to 2005, the monitoring of Changbai Mountain Tianchi V showed a significant increase in earthquake magnitude, topographic variation, frequency and greenhouse gas emissions

associated with the mountain [4,5]. In May 2010, the elevation of the northern slope of the Changbai Mountain Tianchi volcanic cone reversed and decreased by 12.72 mm, breaking the previous pattern of an annual increase of 4 mm. Based on the above monitoring results, the Changbai Mountain Tianchi volcano may be entering an active phase. Therefore, it is necessary to evaluate the hazard of secondary collapse geological hazards caused by volcanic activity in Tianchi, Changbai Mountain.

The development characteristics, distribution areas and inducing factors of different types of geological hazard are different, so the selection of evaluation indicators should equally differ [6,7]. The study area is located in the southeast of the Jilin Province (NE China), and its population is mainly distributed near cities and major transportation roads, while other areas are mostly forested and sparsely populated. According to the analysis of the previous field investigation data, the number of hazards has a positive correlation with human engineering activities. At the same time, the study area is close to the Changbai Mountain crater. Through the analysis of seismic monitoring data acquired over the last 20 years, the frequency of Changbai Mountain volcanic earthquakes has been on the rise, which has a positive impact on the collapse geological hazard in the study area. Therefore, this article selects indicators such as slope, aspect, elevation, curvature, lithology, annual average rainfall, NDVI, distance from faults, and distance from rivers. Additionally, indicators related to human engineering activities such as distance from road and land use type were selected [8]. At the same time, due to the study area being located near the crater of Changbai Mountain, volcanic earthquakes are selected as the inducing factors to assess the collapse geological hazard caused by volcanic earthquakes in the study area.

Volcanic earthquakes and their induced secondary geological disasters not only have a certain impact on ecosystems, but also cause damage to human life and property safety. Many domestic and foreign scholars have been committed to this research. Italian scholar De Vita Sandro [9] found that volcanic activity is an undeniable triggering factor in his research on landslide hazard. American scholar Keefer [10,11] analyzed the data of collapse and landslide hazard caused by earthquakes worldwide, and obtained the distribution patterns of earthquake parameters and collapse and landslide hazard. Japanese scholar Tamura [12,13] analyzed case data of earthquake-induced landslide hazards over the past 100 years in 1978, and obtained the relationship between earthquake parameters such as magnitude and epicenter distance and landslide boundary distance. Huang Yidan [14], a Chinese scholar, and others found that with the increase in earthquake intensity, the development density of collapse geological disasters also increased by interpreting the remote sensing images of the earthquake area and combining with the field survey data. Zhang Jianqiang, Fan Jianrong [15] and others conducted risk analyses on earthquake-induced landslides in Wenchuan County, Sichuan Province by selecting lithology, slope, distance from fault and other indicators.

Previous evaluation methods mostly resort to a single evaluation model. In order to improve the accuracy of the evaluation results of collapse geological hazards in the study area, this article first uses the objective weight method [16,17] to analyze known data, and then combines the subjective weight method [18] to conduct hazard assessment of collapse geological hazards in the study area. At the same time, in the selection of evaluation indicators, comprehensive consideration was given to the terrain and geomorphic characteristics, human engineering activities, special triggering factors, and other aspects of the study area. Indicators such as slope, aspect, elevation, curvature, lithology, annual average precipitation, NDVI, distance from faults, and distance from rivers were selected. At the same time, indicators related to human engineering activities such as distance from roads and land use type were also selected. Combined with the special triggering factor of volcanic earthquakes, the hazard assessment of the secondary geological hazard due to volcanic earthquakes was carried out. The receiver operating characteristic curve (ROC) [19] is used to compare and evaluate the accuracy of the model before and after the combination.

2. Study Area

Changbai Mountain is located in the southeast of Jilin Province, NE China, bordering North Korea to the south and Russia to the east. The study area includes the Changbai Mountain Scenic Area and three surrounding counties, namely, Fusong County, Antu County and Changbai County (Figure 1), with an area of 16,108.96 km^2. Figure 2 shows that during the field investigation, most of the collapse geological hazard points recorded are distributed along the highway.

The study area belongs to the continental humid monsoon climate in the northern temperate zone. Summer is warm and rainy with concentrated precipitation, while winter is cold and long. The annual average temperature is 2–4 °C, and the annual average rainfall is 630~800 mm. The drainage system in the study area is relatively organized, and drainage density is large, with the Yalu, Songhua and Tumen Rivers system. According to the genesis, the geomorphological types can be divided into three categories: volcanic landforms, tectonic denudation landforms and erosion accumulation landforms. The geological structures such as fault zone and fold are mainly distributed in the northeast and southwest of the study area.

The population is mainly distributed in the south of Changbai County, the northeast of Antu County and the central and western parts of Fusong County. At the same time, due to the expansion of the city and the improvement of corresponding infrastructure, more and more people gather in the city and surrounding urban areas, while the population in rural and remote areas is becoming more and more sparse, resulting in a relatively concentrated population distribution. On the other hand, the crater of Changbai Mountain is a volcanic landform with a high elevation, and most of the nearby areas are primeval forests with inconvenient transportation, which are not suitable for human habitation and have a lower population distribution.

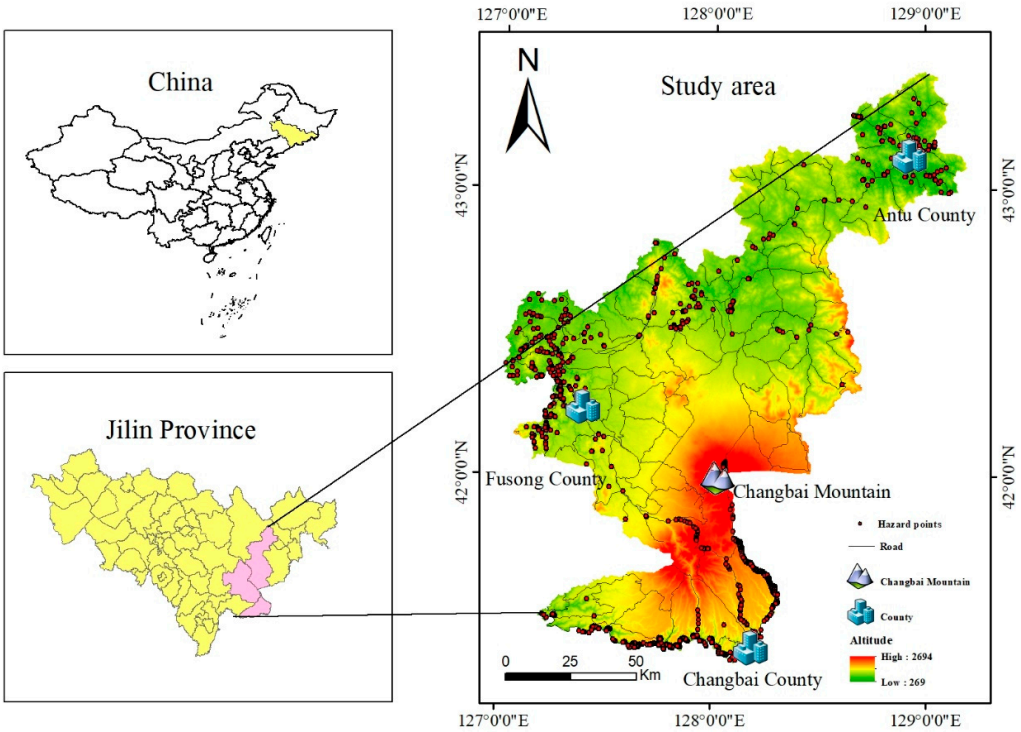

Figure 1. Location map of the study area and distribution of collapse geological hazard points.



Figure 2. Field photos of collapse geological disaster sites in the study area.

3. Methods and Data

This study establishes, analyzes and validates a collapse hazard evaluation model, through the steps of field investigation, data collection, factor correlation analysis and evaluation index selection. The order relation analysis method (G1) and weight of evidence and coefficient of variance (WOE-CV) methods are used to evaluate the collapse geological hazard. Among them, the G1 method is a subjective weight evaluation model improved by the analytic hierarchy process (AHP) [20], which can effectively negate the difference between evaluation indicators. Weight of evidence (WOE) and coefficient of variation (CV) are objective evaluation models. The WOE-CV combination model can optimize the accuracy of the evaluation index weight and improve the accuracy of the evaluation results. The specific process is shown in Figure 3.

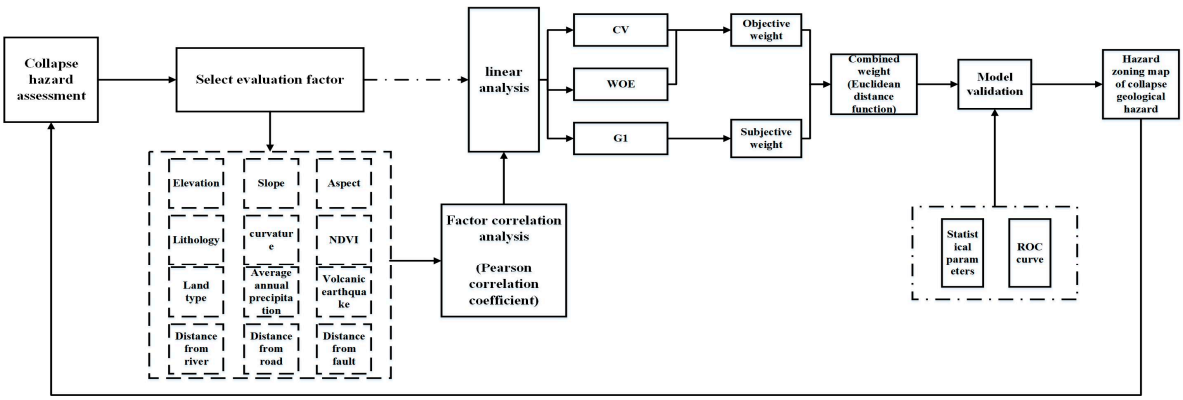

Figure 3. Flow chart of geological hazard analysis and evaluation.

3.1. Index Selection

Collapse phenomena are caused by the joint action of various factors [21]. These include landform, formation lithology and hydrogeology, etc., while the induced factors include volcanic earthquake, rainfall, human engineering activities, etc. Based on these two aspects, according to the characteristics of the study area, this paper selects 12 indicators including NDVI, elevation, slope, curvature, lithology, slope, distance from fault, distance from river, distance from road, annual average precipitation, land use type, and volcanic earthquake to build the collapse geological hazard assessment system (Figure 4).

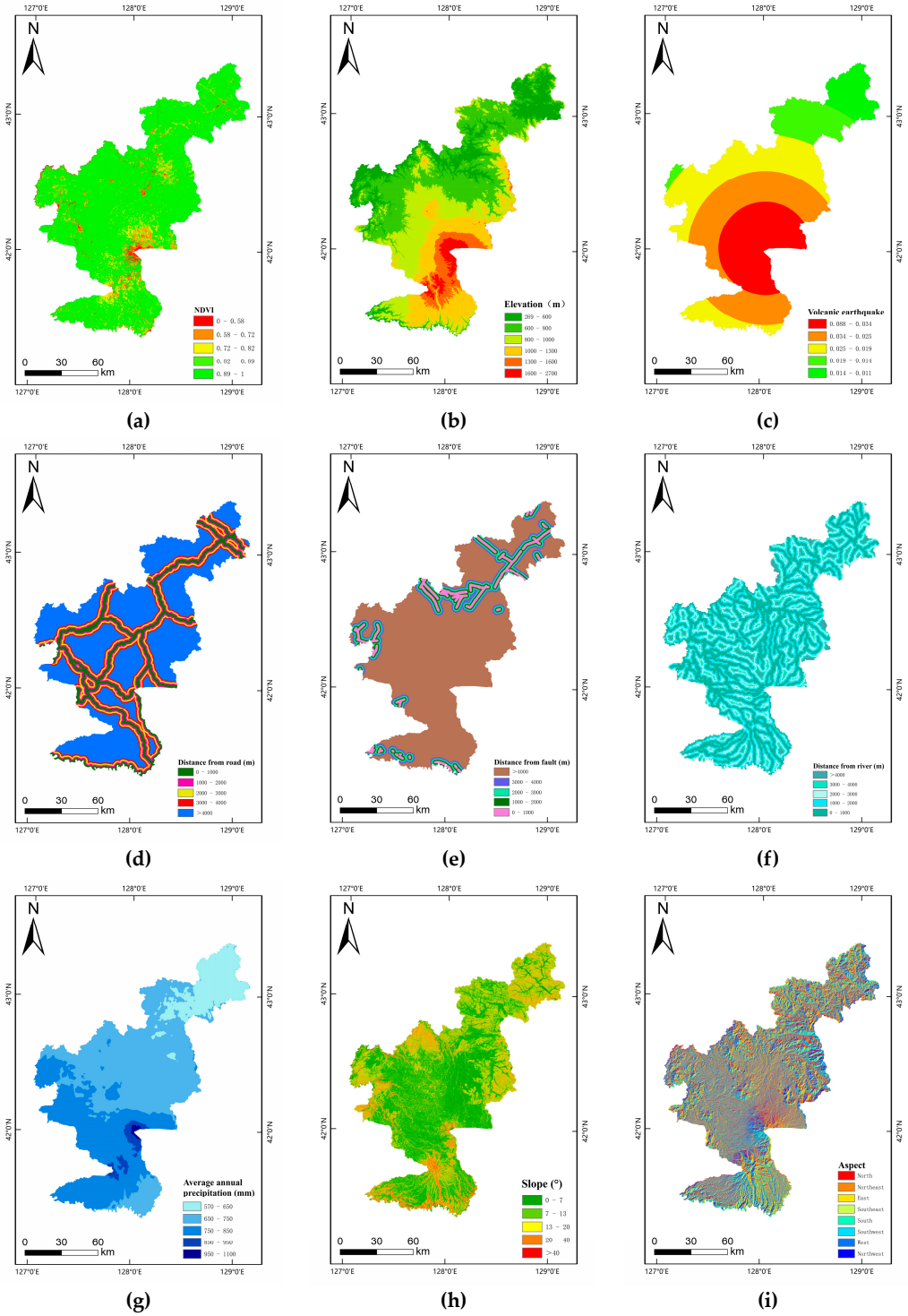

Figure 4. *Cont.*

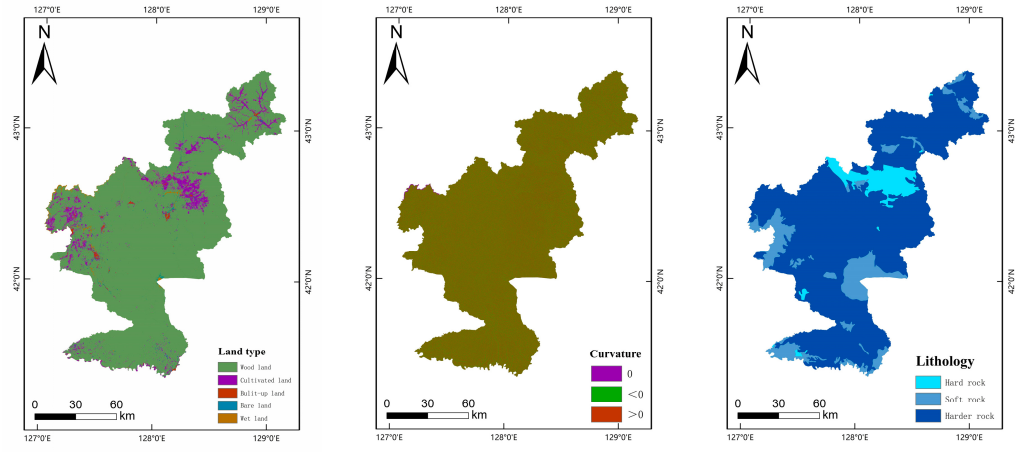

(j) **(k)** **(l)**

Figure 4. Index grading diagram: (**a**) NDVI, (**b**) elevation, (**c**) volcanic earthquake, (**d**) distance from road, (**e**) distance from fault, (**f**) distance from river, (**g**) annual average precipitation, (**h**) slope, (**i**)aspect, (**j**) land type, (**k**) curvature, (**l**) lithology.

In order to analyze the influence degree of Changbai Mountain volcanic earthquakes on the collapse geological hazard in the study area, this paper uses the transcendental probability of the volcanic earthquake intensity greater than VI degrees to express the impact of Changbai Mountain volcanic earthquakes on the stability of the slope in the study area [22]. The specific calculation process is as follows:

Gutenberg Richter recurrence relationship—

$$\lg N(M) = -aM + b \tag{1}$$

where M is the magnitude, N(M) is the cumulative frequency of earthquake occurrence, and a and b are constants.

The relationship between the frequency of volcanic activity and the magnitude of earthquakes associated with volcanic activity [23]

$$\lg N(VEL) = -0.2286H + 1.6286 \tag{2}$$

where H is the magnitude of the earthquake associated with volcanic activity in Changbai Mountain, and N(VEL) is the frequency of volcanic activity.

Through the analysis of the statistical results of earthquake-induced collapse phenomena in various regions, it is found that a seismic intensity of VI is the minimum needed to trigger a collapse. Therefore, the seismic intensity attenuation formula in the study area can be expressed as follows [24]:

$$L = 1.454T - 1.792\ln(G + 16) + 4.493 \tag{3}$$

where L is the earthquake intensity, T is the magnitude at the time of an earthquake, and G is the epicentral distance.

In order to reflect the impact of volcanic earthquakes on the collapse phenomena in the study area, this paper uses the probability of a Changbai Mountain volcanic earthquake of an intensity exceeding VI, and the research time span is 5000 years. The specific formula is as follows:

$$P_{VI} = \frac{\int_K^9 \frac{1}{5000} \times 10^{-0.2286H+1.6286}}{\int_0^9 \frac{1}{5000} \times 10^{-0.2286H+1.6286}} \tag{4}$$

where K represents the magnitude of Changbai Mountain volcanic earthquake required to cause an intensity of VI in the study area, and P_{VI} is the probability that the intensity exceeds VI.

See Table 1 for the selection principles of evaluation indicators.

Table 1. Selection principles of evaluation indicators.

Criteria	Evaluation Indicators	Principle of Selection
Topographic features	Elevation	The vegetation coverage, sunlight exposure area and water catchment of slopes at different elevations, with varying impacts on the rock and soil mass of slopes [25].
	Slope	When the slope exceeds a certain value, it will intensify the gravity effect, easily causing the sliding and collapse of rock layers and soil, especially under the influence of natural disasters such as rainy seasons or earthquakes. Therefore, slope is one of the important factors in the occurrence of collapse geological hazard [26].
	Curvature	The value of the curvature reflects the shape of the slope, including concave slopes, convex slopes, straight slopes, etc. Convex slopes will form a phenomenon of stress concentration at the slope corner, resulting in a decrease in the stability of the slope. The middle part of the concave slope is prone to strong erosion, which is also not conducive to the stability of the slope [27].
	Aspect	Different slope directions are exposed to sunlight and precipitations for different time ranges, which further affects the distribution of vegetation on the slope, the weathering degree of rock and soil, and then the occurrence of geological hazard [28].
Rock and soil mass	Lithology	Formation lithology is the material condition for forming geological hazards. Different formation lithologies have different shear and weathering resistance of rock mass. According to the analysis and statistics of the formation lithology in the study area, geological hazards of collapse mainly occur in hard rock layers [29].
Geological structure	Distance from fault	The strength of the rock and soil around the fault zone is low, and the weathering resistance is weak, which can lead to unstable joint surfaces, and then induce the occurrence of collapse geological hazards [30].
Meteorology and hydrology	Distance from river	Drainage affects the stability of the slope, mainly manifested in scouring and eroding the slope toe, changing the original slope gradient and reducing the strength of the slope [31].
Human engineering activities	Distance from road	Through statistical analysis, it is found that more than 80% of the collapse geological hazard in the study area is affected by human engineering activities. Among them, the construction of roads is the primary factor affecting the stability of slopes, with the excavation, backfilling and stacking of materials during the construction process [32].
Vegetation cover	NDVI	The vegetation normalization index can significantly reflect the spatial distribution of vegetation in the study area. The smaller the NDVI value is, the sparser the vegetation is. The higher the NDVI value is, the higher the vegetation coverage is. Areas with high vegetation cover are less susceptible to erosion than bare areas [33].
	Land use type	The type of land use can objectively reflect the natural environment and human engineering activities in the study area, both of which will affect the occurrence of geological hazards to a certain extent [34,35].
Inducing factor	Volcanic earthquake	The study area is close to the crater of Changbai Mountain, and volcanic activity has occurred frequently in recent years, so volcanic earthquake is selected as the inducing factor for consideration.
	Average annual precipitation	Rainfall may induce slope instability and deformation. Part of the rainfall will form surface runoff and scour the slope surface. At the same time, part of the rain will penetrate into the slope, changing the stress balance inside the slope, and further inducing the occurrence of collapse geological hazards [36].

The research data in this paper mainly consist of spatial vector data, remote sensing image data, and meteorological and hydrological data. The data sources of each evaluation index are shown in Table 2.

Table 2. Data types and sources.

Indicator	Data Source
DEM	Geospatial Date Cloud (http://www.gscloud.cn, accessed on 2 June 2022)
Lithology Distance from fault	National Geological Archives Date Center (http://dc.ngac.org.cn/Home, accessed on 1 January 2021)
Distance from river Distance from road	National Catalogue Service For Geographic Information (https://www.webmap.cn, accessed on 29 April 2022)
NDVI	Google Earth Engine (https://code.earthengine.google.com, accessed on 1 July 2022)
Land type	National Tibetan Plateau Date Center (http://data.tpdc.ac.cn, accessed on 20 July 2021)
Average annual precipitation	China Meteorological Date Service Center (http://data.cma.cn, accessed on 1 January 2022)
Volcanic earthquake	Seismic ground motion parameters zonation map of China GB18306-2015 (https://www.gb18306.net, accessed on 1 June 2022)

The elevation, curvature, slope and aspect are extracted from DEM grid data using ArcGIS software. After obtaining the above data, the ArcGIS software is used for projection transformation and resampling, so that the data can reach a unified resolution and spatial coordinate system. Other information comes from the Jilin Provincial Geological Environment Monitoring Station.

3.2. Building an Evaluation Model

According to the field survey and analysis of historical data in the study area, most of the collapse sites are mainly concentrated in densely populated villages, towns and roads. The reason is that the expansion of towns and the construction of related ancillary facilities have changed the original terrain characteristics. Human factors are an important reason for the occurrence of collapses in the study area. In this paper, the subjective weight method (G1 method) and the objective weight method (WOE-CV) are combined to evaluate the collapse geological hazard in the study area based on remote sensing satellite images, field survey data and historical data of the study area. On one hand, the ranking of index importance and weight calculation are more consistent with the actual situation in the study area through the order relation analysis method; on the other hand, the weight of evidence is used to obtain the original data to compensate for the impact of subjective evaluation, making the final evaluation results more accurate and reasonable. Finally, the two weights are combined using the Euclidean distance function to improve the accuracy of the model.

3.2.1. Order Relation Analysis Method (G1 Method)

Order relation analysis (G1) is a subjective evaluation model that is mainly used to rank the importance of two adjacent indicators by means of expert scoring, so as to further determine the weight of each index. When too many evaluation indicators are selected, the G1 method can, to a certain extent, avoid the disadvantage that the weight is difficult to be determined due to too many evaluation indicators and a large amount of data, and effectively avoid the problem of excessive differences between indicators. The calculation process is clear, which greatly simplifies the calculation steps [37]. The algorithm steps of the G1 method are as follows:

(1) Deterministic order relation

Assuming that the evaluation object is A, the corresponding evaluation indicators are named X_1, X_2, X_3 … X_m. If the importance of X_i is not inferior to X_j based on a certain evaluation criterion or evaluation object, it is expressed as $X_i \geq X_j$ (the symbol $\geq$ means not inferior to).

Based on a certain criterion or evaluation object, if the following relationships exist between indicators, it is said that a relationship of importance between evaluation indicators $X_1, X_2, X_3 \ldots X_m$ is determined.

$$X_1 * \geq X_2 * \geq \ldots \geq X_m *$$

The specific operation steps are as follows:

Assume there are m factors.

The decision-maker first selects the most important factor from the m factors and marks it as X_1 *.

The decision-maker continues to select the most important factor from the remaining $m - 1$ factors and mark it as X_2 *.

Repeat the above action until all the factor markers are completed.

(2) Judge the importance ratio

Assume that the ratio of importance of evaluation index X_{k-1} to X_k is W_{k-1}/W_k, and $W_{k-1}/W_k = r_k$ (k = m, $m - 1$, $m - 2$, . . ., 3, 2).

r_k is a mood operator, and the nine-level operator method is commonly used in China. The importance assignment of specific indicators is illustrated in Table 3.

Table 3. Index importance assignment table.

r_k	Explain
1.0	X_{k-1} and X_k are equally important
1.1	X_{k-1} and X_k are between equally important and slightly important
1.2	X_{k-1} is slightly more important than X_k
1.3	X_{k-1} and X_k are between slightly important and obviously important
1.4	X_{k-1} is obviously more important than X_k
1.5	X_{k-1} and X_k are between obviously important and strongly important
1.6	X_{k-1} is strongly more important than X_k
1.7	X_{k-1} and X_k are between strongly important and extremely important
1.8	X_{k-1} is extremely more important than X_k

(3) Calculation of weight coefficient

The expert gives the assignment of r_k, and uses the following formula to calculate the weight value W of the index. The calculation formula is as follows:

$$W_m = \left(1 + \sum_{k=2}^{m} \prod_{i=k}^{m} ri\right)^{-1} \quad (5)$$

Suppose there are m indicators in total, and W_m represents the weight value of the m-th indicator. The subjective weight of other $m - 1$ indicators is calculated by the following formula:

$$w_{k-1} = r_k w_k (k = m, m-1, \ldots 3, 2) \quad (6)$$

3.2.2. Weight of Evidence (WOE)

Weight of evidence is an objective weight calculation method, which is mainly driven by the data of Bayesian conditional probability, and conducts superposition analysis by collecting various existing information. The model covers image analysis, mathematical statistics, artificial intelligence, etc., and is organically combined to effectively predict the study area based on the GIS platform. Weight of evidence was initially used in the prediction of mineral target area [38], and then gradually applied by some scholars to the evaluation of collapse and landslide geological hazards.

(1) Calculate a prior probability

The prior probability is expressed as the probability of collapse in the study area, which is calculated by the distribution of existing hazard points. The author uses ArcGIS to divide the study area into cells; the cell division standard is to divide the study area into several grid cells with the same shape and equal areas. In order to maximize the accuracy of the data, according to the resolution of the original data, this paper divides the whole study area into cells with an area of 30 m × 30 m. The regional statistical tool in the regional analysis tool is used to conduct joint statistics on the existing hazard point data and the divided cell data to determine the number of units containing geological hazard points.

Assuming that the study area has a total of A cells, the number of cells containing geological hazard points is determined to be N through the zoning statistical function, then the formula for calculating the prior probability is as follows:

$$\mathrm{P(D)} = \frac{A}{N} \tag{7}$$

A is the total number of cells in the study area, N is the number of cells containing collapse geological hazard points, and P(D) is a prior probability.

(2) Weight calculation

We assume that the whole study area is divided into A grid cells with the same size and area within the study area. These grid cells are classified and counted according to the classification of influence factors. Among them, the number of grids with geological hazards is recorded as D, the number of grids without geological hazards is $\overline{\mathrm{D}}$, and B is the number of grids with geological hazards under a certain impact factor classification. The number of grids without geological hazards under this impact factor classification is $\overline{\mathrm{B}}$. For any index weight classification, the weight is calculated as:

$$\begin{cases} W^{+} = ln\dfrac{P\left(\dfrac{B}{D}\right)}{P\left(\dfrac{B}{\overline{D}}\right)} \\ W^{-} = ln\dfrac{P\left(\dfrac{\overline{B}}{D}\right)}{P\left(\dfrac{\overline{B}}{\overline{D}}\right)} \end{cases} \tag{8}$$

where W^{+} represents the weight value of the area where the impact factor exists, and W^{-} represents the weight value of the area where the impact factor does not exist. The larger the value of W^{+}, the closer the relationship with the occurrence of hazards. The smaller the value of W^{-}, the less close the relationship with the occurrence of hazards. P represents conditional probability, that is, the probability of occurrence and non-occurrence of geological hazards under different conditions.

$$\mathrm{C} = W^{+} - W^{-} \tag{9}$$

In the formula, C is the comprehensive weight value, and the larger the C value, the higher the contribution of the evidence factor to the occurrence of hazard. The lower the C value, the lower the contribution of the evidence factor to the occurrence of hazard.

(3) Calculate a posteriori probability

For m evidence factors, the probability of geological hazards occurring in any unit K in the study area is:

$$\mathrm{lnR} = W_0 + \sum_{i}^{m} W_i^k (i = 1, 2, \ldots, m) \tag{10}$$

where $W_0 = \ln[P_0/(1-P_0)]$, P_0 is a prior probability, and W_i^k is the weight value of the ith factor.

Calculation of posterior probability:

$$P_{(A)} = R/(1+R) \tag{11}$$

The magnitude of the posterior probability value reflects the hazard of geological hazards. The greater the posterior probability is, the higher the hazard is. The smaller the posterior probability is, the lower the hazard is. See Table 4 for the distribution of evidence weight factors and their weight values.

Table 4. Distribution and weight value of evidence weight factors.

Evidence Factors	Classification	Number of Cells	Number of Hazards	W^+	W^-	C	$P_{(A)}$
NDVI	0–0.58	313,974	63	1.47667	−0.05182	1.52849	0.00020065
	0.58–0.72	668,216	144	1.54806	−0.12761	1.67567	0.00021550
	0.72–0.82	1,425,234	204	1.13882	−0.16501	1.30383	0.00014313
	0.82–0.89	3,273,150	278	0.61684	−0.16813	0.78497	0.00008493
	0.89–1	15,634,670	288	−0.91162	0.97320	−1.88482	0.00001842
Distance from fault (m)	0–1000	1,180,622	109	0.70029	−0.06132	0.76160	0.00009232
	1000–2000	1,151,732	77	0.37750	−0.02655	0.40404	0.00006686
	2000–3000	1,082,263	67	0.30059	−0.01893	0.31952	0.00006191
	3000–4000	1,021,729	54	0.14243	−0.00774	0.15017	0.00005285
	>4000	16,878,898	670	−0.14386	0.41198	−0.55583	0.00003969
Elevation (m)	269–600	3,311,114	455	1.09804	−0.45801	1.55605	0.00013742
	600–800	7,462,661	235	−0.37541	0.15582	−0.53123	0.00003149
	800–1000	4,965,081	73	−1.13707	0.18754	−1.32460	0.00001470
	1000–1300	3,650,234	91	−0.60902	0.09007	−0.69909	0.00002493
	1300–1600	1,322,724	74	0.19932	−0.01470	0.21402	0.00005595
	1600–2700	603,430	49	0.57192	−0.02274	0.59465	0.00008120
Distance from river (m)	0–1000	8,966,141	734	0.58003	−0.84561	1.42564	0.00008186
	1000–2000	6,678,777	134	−0.82619	0.22840	−1.05458	0.00002006
	2000–3000	3,607,311	75	−0.79056	0.10554	−0.89611	0.00002079
	3000–4000	1,476,359	26	−0.95657	0.04481	−1.00138	0.00001761
	>4000	586,656	8	−1.21234	0.01969	−1.23203	0.00001364
Volcanic earthquake	0.088–0.034	4,741,785	200	−0.08316	0.02257	−0.10574	0.00004218
	0.034–0.025	6,448,480	173	−0.53564	0.16542	−0.70105	0.00002683
	0.025–0.019	5,894,248	456	0.52348	−0.30506	0.82854	0.00007736
	0.019–0.014	2,504,709	27	−1.44743	0.09699	−1.54442	0.00001078
	0.014–0.011	1,726,022	121	0.42493	−0.04778	0.47271	0.00007010
Slope (°)	0–7	7,842,641	89	−1.39604	0.36327	−1.75931	0.00001135
	7–13	6,599,765	156	−0.66226	0.19657	−0.85883	0.00002364
	13–20	3,953,879	175	−0.03498	0.00780	−0.04277	0.00004426
	20–40	2,739,782	382	1.11257	−0.35836	1.47093	0.00013943
	>40	179,177	175	3.06003	−0.18894	3.24898	0.00097669
Aspect	North	2,877,596	72	−0.60537	0.06848	−0.67385	0.00002502
	Northeast	2,689,788	109	−0.12318	0.01660	−0.13978	0.00004052
	East	2,621,511	153	0.24164	−0.03908	0.28072	0.00005836
	Southeast	2,277,835	210	0.69886	−0.12899	0.82785	0.00009219
	South	2,580,040	163	0.32090	−0.05351	0.37441	0.00006318
	Southwest	2,652,967	142	0.15509	−0.02414	0.17923	0.00005352
	West	2,901,265	78	−0.53352	0.06311	−0.59663	0.00002688
	Northwest	2,714,242	50	−0.91158	0.08368	−0.99526	0.00001842
Curvature	<0	10,199,533	534	0.13300	−0.13986	0.27286	0.00005236
	0	1,168,179	36	−0.39701	0.01882	−0.41583	0.00003082
	>0	9,947,532	407	−0.11358	0.08980	−0.20338	0.00004091
Land type	Wood land	19,448,699	662	−0.29759	1.30354	−1.60113	0.00003404
	Cultivated land	1,383,114	107	0.52346	−0.04891	0.57236	0.00007736
	Bulit-up land	159,839	79	2.37842	−0.07679	2.45521	0.00049425
	Bare land	192,787	117	2.58384	−0.11847	2.70231	0.00060689
	Wet land	130,805	12	0.69394	−0.00620	0.70014	0.00009174
Lithology	Harder rock	17,130,568	638	−0.20760	0.56954	−0.77714	0.00003724
	Soft rock	2,874,907	308	0.84908	−0.23383	1.08291	0.00010713
	Hard rock	1,309,769	31	−0.66095	0.03117	−0.69212	0.00002367
Distance from road (m)	0–1000	2,615,504	669	1.71947	−1.02350	2.74298	0.00025578
	1000–2000	2,195,692	66	−0.42192	0.03877	−0.46069	0.00003006
	2000–3000	1,988,314	38	−0.87479	0.05825	−0.93305	0.00001911
	3000–4000	1,734,351	23	−1.24024	0.06105	−1.30128	0.00001326
	>4000	12,781,383	181	−1.17459	0.71054	−1.88513	0.00001416
Average annual precipitation (mm)	570–650	2,987,969	137	0.00032	−0.00005	0.00038	0.00004585
	650–750	10,682,978	411	−0.17513	0.14964	−0.32477	0.00003847
	750–850	7,096,453	379	0.15288	−0.08604	0.23893	0.00005341
	850–950	483,402	31	0.33585	−0.00930	0.34515	0.00006413
	950–1100	64,442	19	1.86161	−0.01661	1.87823	0.00029484

Because the final result of the weight of evidence is the posterior probability of the secondary evaluation factor, the weight value of the primary evaluation factor is considered. Therefore, based on the weight of evidence, this paper uses the coefficient of variation method to calculate the weight value of the first-level evaluation factor of collapse hazard.

3.2.3. Coefficient of Variance (CV)

The coefficient of variation, also known as the standard deviation rate, is to calculate the standard deviation and average value of a group of information by using the information contained in each factor, and use the ratio of the two as an objective weighting method for the weight value of the influence factor. The calculated weight value can effectively reflect the gap of evaluation indicators [39].

The specific calculation steps are as follows:

(1) Standardized treatment.

Because the dimensions of each factor are different, in order to avoid the impact on the results, the first step is to standardize the first-level evaluation indicators as dimensionless.

$$\text{Positive indicators}: \ A_{ij} = \frac{X_{ij} - (min)X_i}{(max)X_i - (min)X_i} \tag{12}$$

$$\text{Negative indicators}: \ A_{ij} = \frac{(max)X_i - X_{ij}}{(max)X_i - (min)X_i} \tag{13}$$

A_{ij} is the i-th, standardized value of the j-type evaluation factor, A_{ij} is the i-th, original value of the j-type evaluation factor, $(min)X_i$ is the minimum value of the i-th evaluation factor, and $(max)X_i$ is the maximum value of the i-th evaluation factor.

(2) Calculate the coefficient of variation and weight value.

Average:

$$\overline{X_j} = \frac{1}{n}\sum_{i=1}^{n} x_{ij} \tag{14}$$

Standard deviation:

$$S_j^2 = \frac{1}{n-1}\sum_{i=1}^{n}\left(x_{ij} - \overline{X_j}\right)^2 \tag{15}$$

Coefficient of variation:

$$C_v = S_j / \overline{X_j} \tag{16}$$

Weight value:

$$\omega_j = C_v / \sum_{j=1}^{p} C_v \tag{17}$$

On the basis of the posterior probability of the existing second-level evaluation indicators, combined with the coefficient of variation method, the weight value of each first-level evaluation index is further calculated, as shown in Table 5.

3.2.4. Combination Weight

For the evaluation of collapse geological hazards in the study area, first, according to the actual situation in the study area, fully consider the characteristics of the evaluation index themselves, and calculate the subjective weight. Secondly, consider the existing data information, objectively evaluate the existing data within the study area, and reflect the data characteristics of each evaluation index through objective weight.

In order to ensure that the evaluation results are both subjective and objective, the two weight calculation methods are combined. On the basis of the Lagrangian function and European distance function, a combined weight model is constructed to calculate the combined weight value.

Table 5. First-level evaluation index weight value.

Evaluation Factor	Average	Standard Deviation	Coefficient of Variation	Weight Value
Land type	5,421,204.4	7,116,344.351	1.312686965	0.142485503
NDVI	8,158,410.4	4,468,700.668	0.547741588	0.059454568
Aspect	14,315,560.75	5,201,882.555	0.363372602	0.039442251
Elevation	14,400,680.5	11,112,883.19	0.771691532	0.083763197
Slope	13,640,479.6	7,542,532.487	0.552952147	0.060020147
Distance from fault	8,808,624.4	4,764,803.379	0.540924799	0.05871464
Volcanic earthquake	22,137,892	17,042,856.53	0.769850017	0.08356331
Lithology	44,195,626	42,385,456.04	0.959041875	0.104099125
Distance from river	30,206,968.2	29,026,962.87	0.960935989	0.104304721
Curvature	51,661,842	36,488,511.95	0.706295218	0.076664759
Distance from road	17,785,890	12,496,151.36	0.702587914	0.07626235
Average annual precipitation	11,986,172.4	12,282,169.97	1.02469492	0.11122543

(1) Build a combination weight model.

$$W_s = aW_x + bW_y \tag{18}$$

where W_s is the combined weight value, W_x and W_y are the subjective weight value and objective weight value, respectively, and a and b are the optimization coefficients of subjective weight and objective weight, respectively.

(2) Based on the Euclidean distance function, establish the equations.

$$\begin{cases} H_{(W_{xj},W_{yj})} = \sqrt{\dfrac{\sum_{j=1}^{n}\left(W_{xj} - W_{yj}\right)^2}{2}} \\ {H_{(W_{xj},W_{yj})}}^2 = (a-b)^2 \\ a + b = 1 \end{cases} \tag{19}$$

(3) Calculate the combined weight value.

According to the weight value calculated by the subjective weight G1 and objective weight WOE-CV, the combined weight value of each evaluation index is calculated by simultaneous equations. See Table 6 for details.

Table 6. Combination weight calculation results.

Evaluation Factor	Subjective Weight	Objective Weight	Combined Weight
Land type	0.178790582	0.142485503	0.159863837
NDVI	0.112872842	0.059454568	0.08502456
Aspect	0.054433277	0.039442251	0.04661808
Elevation	0.045361064	0.083763197	0.065381056
Slope	0.148992152	0.060020147	0.102608822
Distance from fault	0.094060702	0.05871464	0.075633916
Volcanic earthquake	0.022367388	0.08356331	0.054270352
Lithology	0.065319932	0.104099125	0.085536495
Distance from river	0.078383918	0.104304721	0.091897081
Curvature	0.034893126	0.076664759	0.056669723
Distance from road	0.135447411	0.07626235	0.104592759
Average annual precipitation	0.029077605	0.11122543	0.07190332

4. Result and Discussion

4.1. Evaluation Index Correlation Analysis

In the selection of an evaluation index for collapse geological hazards, if the correlation coefficient of the two groups of evaluation indices is too high, it will have a great impact on the final result. Therefore, in order to ensure the independence and objectivity of each evaluation index, improve the accuracy of the prediction model, and reduce the interaction between the factors, the Pearson correlation coefficient method is used to analyze the correlation of the evaluation index.

Correlation coefficient, also known as product correlation coefficient, is a linear correlation coefficient that can be used to reflect the degree of correlation between two continuous variables with normal distribution. The size of the correlation coefficient reflects the strength of the correlation between indexes. When the correlation coefficient between indices is less than 0.6, it is considered that the correlation is weak and has little impact on the accuracy of the evaluation model [40].

In this paper, the ArcGIS software's spatial Analyst Toolset multivariate analysis band set statistical tool is used to conduct statistical analysis on the grid data of the influencing factors, and calculate the covariance and correlation matrix. The origin drawing software is used to draw a hot spot map of the index correlation, and the results are shown in Figure 5.

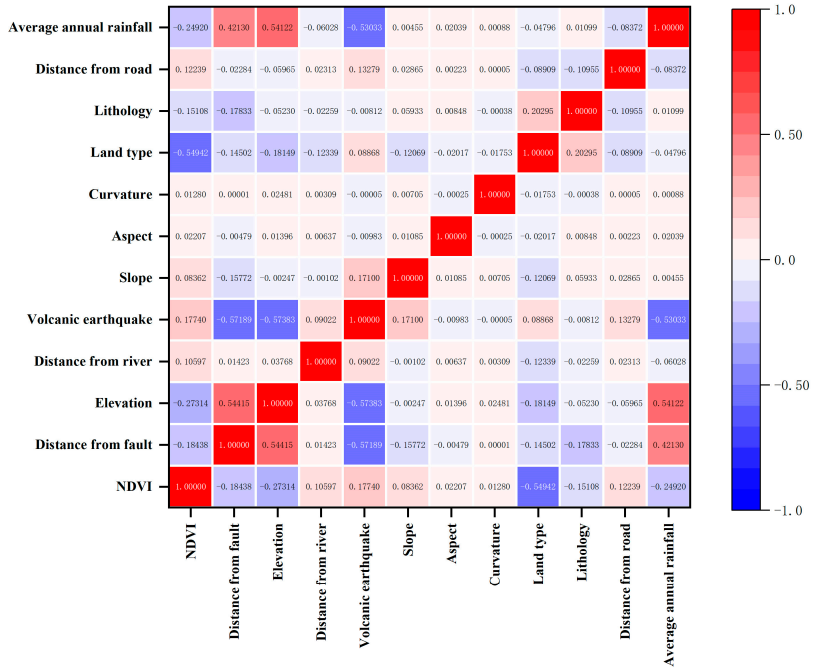

Figure 5. Hot spot map of index correlation.

According to the analysis and statistics of various data in the figure, the correlation coefficient between volcanic earthquake and elevation and distance is slightly higher, about 0.57. The correlation coefficients among other evaluation indexes are less than 0.6, which indicates that the correlation and influences of the selected evaluation indexes are not significant.

4.2. Comparative Analysis of Evaluation Models

The results show that the hazard point density of the three models increases with the increase in hazard grade. At the same time, through the horizontal comparison of hazard point density, it can be found that in the high- and very high-hazard areas, the hazard point density was significantly improved after the combination of the G1 method and the WOE-CV method through the Euclidean distance function. It shows that the accuracy of

the combined prediction model is higher, and the prediction result is more reasonable, as shown in Table 7.

Table 7. Correlation analysis of hazard points.

Classification	Area (km^2)			Number of Hazard Points			Density of Hazard Points (km^{-2})		
	G1	WOE-CV	Combined Weight	G1	WOE-CV	Combined Weight	G1	WOE-CV	Combined Weight
Low	2947	2346	3098	26	38	23	0.009	0.016	0.007
Middle	5934	6797	7080	145	130	97	0.024	0.019	0.014
High	4931	6436	5424	235	432	465	0.048	0.067	0.086
very high	2211	444	421	571	377	392	0.258	0.850	0.932

Combined with Figures 1, 3 and 5, the numbers of hazard points in high- and very-high hazard areas predicted based on the combined weight model are relatively dense, mainly distributed in the northeast and west of the study area and along the national highway of Changbai County, showing a zonal distribution, which is consistent with the actual survey results. The distribution of faults and roads in this area is relatively dense, and the geological environment is poor, which is the main reason for the frequent occurrence of environmental geological hazards in the study area.

4.3. Hazard Map Analysis of Collapse Geological Hazard

According to the calculation results of the combined weights, the grid data of each evaluation index are superposed and summarized using the grid calculator tool through ArcGIS, and finally a hazard assessment zoning map of collapse geological hazards in the study area is obtained. In order to more intuitively reflect the distribution of hazard areas in the study area, the hazard level in the study area is divided into four levels—low, medium, high and very high—by the natural breakpoint classification method. See Figure 6 for details.

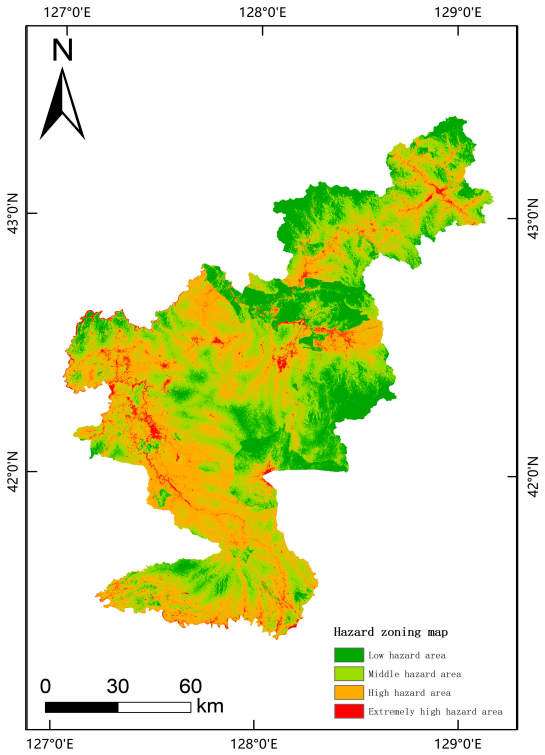

Figure 6. Hazard zoning map of the study area.

The statistical results of each zone are used to conduct statistical analysis on the classified area, area proportion, number of hazard points and proportion of hazard points in each zone, and the following table is obtained. See Table 8 for specific results.

Table 8. Statistical table of partition results.

Classification	Area (km^2)	Proportion (%)	Number of Hazard Points	Proportion of Hazard Points (%)
Low-hazard area	3097.64	19.33	23	2.35
Middle-hazard area	7080.22	44.19	97	9.93
High-hazard area	5423.77	33.85	465	47.59
Very-high hazard area	420.72	2.63	392	40.13

The results show that the high-hazard area and very-high hazard area account for 36.48% of the total area of the study area, and the number of hazard points in the high-hazard area and very high-hazard area accounted for 87.72% of the total number of hazard points in the study area; 47.59% of the collapse hazard points are located in high-hazard areas, and 40.13% of the hazard points are located in very-high hazard areas, indicating that the accuracy of the model is high. From the distribution of hazard levels, the medium- and low-hazard areas are mainly distributed in the north of the Changbai Mountain Scenic Area and the northwest of Changbai County, while the high-hazard area and very high-hazard area are mainly distributed near the national and provincial trunk roads and densely populated areas in the study area. This further shows that the collapse geological hazards in the study area are mainly affected by human engineering activities.

4.4. Model Accuracy Verification

The receiver operating characteristic curve is an index reflecting the sensitivity and specificity of continuous variables based on a series of different binary data, which can effectively negate the impact of human factors on the accuracy of results, and has good objectivity [41]. In the last several years, it has been widely used to evaluate the accuracy of geological hazard prediction models. The area of the ROC curve is expressed by the AUC value, which ranges from 0 to 1. When the value is closer to 1, the accuracy of the model is higher.

In this paper, observation samples and model values of the G1, WOE-CV and combined weight model are used as data sources, and are imported into the SPSS software for ROC curve analysis, while the AUC values are calculated. The results are shown in Figure 7.

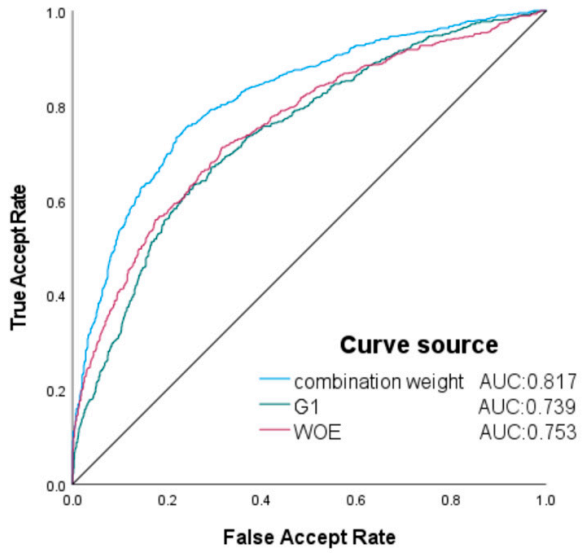

Figure 7. ROC curve.

The AUC values of the G1 and WOE-CV methods are 0.739 and 0.753, respectively, and the AUC value of the combination is 0.817, which shows that the accuracy of the model is significantly improved by the combination of subjective and objective objects through the European distance function.

5. Conclusions

Based on an actual filed survey of the study area, at the same time, taking into account the various anomalies that have occurred around the Changbai Mountain Tianchi volcano in the study area in recent years, this article selected 12 indicators, namely, slope, aspect, elevation, curvature, lithology, land use type, NDVI, annual average precipitation, volcanic earthquake, distance from road, river and fault, to evaluate collapse geological hazards in the study area, and drew a hazard zoning map. The transcendental probability of Changbai Mountain volcanic earthquakes greater than VI was used to reflect the relationship between Changbai Mountain volcanic earthquakes and collapse geological hazards in the study area. Then, the G1 and WOE-CV models were combined, and the models before and after the combination were compared to draw the following inferences.

The AUC value of the combined model reached 0.817, which is significantly higher than that of the previous G1 method (0.739) and the WOE-CV method (0.753), indicating that the combined model is more accurate and can objectively and effectively reflect the actual situation of the study area. At the same time, it also shows that the evaluation method based on the combined subjective and objective weights is suitable for the hazard analysis of collapse geological hazards in the study area.

According to the collapse geological hazard map established according to the combined weight model, the low-, medium-, high- and very high-hazard areas account for 19.33%, 44.19%, 33.85% and 2.63% of the total area of the study area, respectively. At the same time, high-hazard areas and very high-hazard areas account for 87.72% of the total number of known collapse geological hazard points in the study area; 47.59% of the collapse hazard points are located in the high-hazard area, and 40.13% of the hazard points are in the very high-hazard area.

Based on the in-field photos and hazard zoning maps of the hazard points, it can be inferred that most of the hazard points are mainly distributed near the highway, with some being important transportation arteries. Once a geological hazard occurs, it will cause road damage, affect traffic, and endanger the safety of pedestrians passing by. There are also some collapse geological hazard points distributed around villages and farmland. Although there are some warning signs and protective measures are enforced on this site, investigations have found that some protective works, such as gabion retaining walls and defense nets, are in disrepair, with weakened protective functions and significant safety hazards.

By comparing the hazard zoning map and the distribution of known geological hazards of collapse in the study area, it is found that low- and medium-hazard areas are far away from densely populated areas, such as cities and towns, while high-hazard areas and very high-hazard areas are mainly distributed in densely populated areas. Once a collapse geological hazard occurs, it will cause huge economic and property losses. Therefore, it is recommended to take corresponding protective measures for key areas, strengthen hazard monitoring and attach importance to the deployment of hazard prevention and mitigation work.

In the process of calculating the volcanic earthquake evaluation index in this study, the earthquake intensity attenuation formula in eastern China is used, which is employed across a relatively wide range, and there may be certain deviations in the calculation accuracy. At the same time, in the process of acquiring remote sensing images, there are problems such as the large time span and insufficient clarity of the image data. Therefore, in future research work, the applicable range of the seismic intensity attenuation formula can be further narrowed to support more comprehensive data analyses and more accurate results. At the same time, advanced remote sensing monitoring methods, such as synthetic aperture radar

(SAR), unmanned aerial vehicle remote sensing technology, system integration technology, etc., can be used to eliminate data biases or errors, improve the efficiency of data analysis, and thus improve the accuracy of geological hazard assessment results.

Author Contributions: Writing—original draft preparation, methodology, formal analysis, and validation: Zengkai Pan and Qiuling Lang; writing—review and editing: Yichen Zhang, Jiquan Zhang, Chenglong Yu and Chenyang Wu. All authors have read and agreed to the published version of the manuscript.

Funding: This research received no external funding.

Data Availability Statement: Not applicable.

Acknowledgments: The authors would like to thank the editor and anonymous reviewers for their comments and suggestions, which helped to significantly improve this paper.

Conflicts of Interest: The authors declare no conflict of interest.

References

1. Mulero, D.L.; Njå, O.; Fernández, C.L. Landslide risk management in the urban development of sandnes (norway). *Int. Arch. Photogramm. Remote Sens. Spat. Inf. Sci.* **2018**, *XLII-3/W4*, 327–334. [CrossRef]
2. Cui, P.; Peng, J.; Shi, P.; Tang, H.; Ouyang, C.; Zou, Q.; Liu, L.; Li, C.; Lei, Y. Scientific challenges of research on natural hazards and disaster risk. *Geogr. Sustain.* **2021**, *2*, 216–223. [CrossRef]
3. Wu, X.; Wang, Z.; Gao, G.; Guo, J.; Xue, P. Disaster probability, optimal government expenditure for disaster prevention and mitigation, and expected economic growth. *Sci. Total Environ.* **2019**, *709*, 135888. [CrossRef]
4. Chen, Q.-F.; Ai, Y.; Chen, Y. Overview of deep structures under the Changbaishan volcanic area in Northeast China. *Sci. China Earth Sci.* **2019**, *62*, 935–952. [CrossRef]
5. Liu, G.M.; Sun, Y.T.; Li, T.; Zhong, G.P.; Gong, Z.; Su, X.T. The geochemical monitoring of volcanic gases in the Tianchi Area of the Changbaishan mountains and discussion of their data processing methods. *Bull. Mineral. Petrol. Geochem.* **2018**, *37*, 621–628+795. [CrossRef]
6. Pederson, C.A.; Santi, P.M.; Pyles, D.R. Relating the compensational stacking of debris-flow fans to characteristics of their underlying stratigraphy: Implications for geologic hazard assessment and mitigation. *Geomorphology* **2015**, *248*, 47–56. [CrossRef]
7. Yanar, T.; Kocaman, S.; Gokceoglu, C. Use of Mamdani Fuzzy Algorithm for Multi-Hazard Susceptibility Assessment in a Developing Urban Settlement (Mamak, Ankara, Turkey). *ISPRS Int. J. Geo-Inf.* **2020**, *9*, 114. [CrossRef]
8. Gill, J.C.; Malamud, B.D. Anthropogenic processes, natural hazards, and interactions in a multi-hazard framework. *Earth-Sci. Rev.* **2017**, *166*, 246–269. [CrossRef]
9. de Vita, S.; Sansivero, F.; Orsi, G.; Marotta, E. Cyclical slope instability and volcanism related to volcano-tectonism in resurgent calderas: The Ischia island (Italy) case study. *Eng. Geol.* **2006**, *86*, 148–165. [CrossRef]
10. Miles, S.B.; Keefer, D.K. Evaluation of CAMEL—Comprehensive areal model of earthquake-induced landslides. *Eng. Geol.* **2008**, *104*, 1–15. [CrossRef]
11. Keefer, D.K.; Wasowski, J.; Del Gaudio, V. Special issue from the European Geosciences Union Symposium on landslides induced by earthquake and volcanic activity. *Eng. Geol.* **2006**, *86*, 85–86. [CrossRef]
12. ElGharbawi, T.; Tamura, M. Coseismic and postseismic deformation estimation of the 2011 Tohoku earthquake in Kanto Region, Japan, using InSAR time series analysis and GPS. *Remote Sens. Environ.* **2015**, *168*, 374–387. [CrossRef]
13. Tamura, J.; Okada, T. Ambient noise tomography in the Naruko/Onikobe volcanic area, NE Japan: Implications for geofluids and seismic activity. *Earth Planets Space* **2016**, *68*, 5. [CrossRef]
14. Huang, Y.-D.; Yao, L.K.; Guo, C.W.; Guo, H.Q. Distribution law of earthquake-induced collapse and landslide in intensity regions VII to IX. *J. Basic Sci. Eng. Ing.* **2015**, *23*, 92–102.
15. Zhang, J.Q.; Fan, J.R.; Yan, D.; Guo, F.F.; Su, F.H. Sensitivity evaluation to the earthquake-induced landslide and collapse: A case study of Beichuan county, Sichuan province. *J. Sichuan Univ. (Eng. Sci. Ed.)* **2009**, *41*, 140–145. [CrossRef]
16. Lin, J.; Chen, W.; Qi, X.; Hou, H. Risk assessment and its influencing factors analysis of geological hazards in typical mountain environment. *J. Clean. Prod.* **2021**, *309*, 127077. [CrossRef]
17. Koradecka, D.; Pośniak, M.; Widerszal-Bazyl, M.; Augusty Nska, D.; Radkiewicz, P. A comparative study of objective and subjective assessment of occupational risk. *Int. J. Occup. Saf. Ergon.* **2010**, *16*, 3–22. [CrossRef]
18. Tan, Q.; Bai, M.; Zhou, P.; Hu, J.; Qin, X. Geological hazard risk assessment of line landslide based on remotely sensed data and GIS. *Measurement* **2021**, *169*, 108370. [CrossRef]
19. Gorsevski, P.V.; Gessler, P.E.; Foltz, R.B.; Elliot, W.J. Spatial prediction of landslide hazard using logistic regression and ROC analysis. *Trans. GIS* **2006**, *10*, 395–415. [CrossRef]
20. Zheng, Q.; Lyu, H.M.; Zhou, A.; Shen, S.L. Risk assessment of geohazards along Cheng-Kun railway using fuzzy AHP incorporated into GIS. *Geomat. Nat. Hazards Risk* **2021**, *12*, 1508–1531. [CrossRef]

21. Chen, L.; Wang, W.; Zhang, W. Risk Evaluation of Regional Collapses Geological Hazard Based on D-S Evidence Theory-A case study of Haiyuan active fault belt in Ningxia Province. *Energy Procedia* **2012**, *16*, 371–376. [CrossRef]
22. Sun, X.; Yu, C.; Li, Y.; Rene, N.N. Susceptibility Mapping of Typical Geological Hazards in Helong City Affected by Volcanic Activity of Changbai Mountain, Northeastern China. *ISPRS Int. J. Geo-Inf.* **2022**, *11*, 344. [CrossRef]
23. Liu, X. Hazard Assessment of Landslide and Collapse Induced by Volcanic Eruption in Changbai Mountains. Master's Thesis, Jilin University, Changchun, China, 2016.
24. Ding, Y.-H. The Relationship between Earthquake Collapse and Seismic Parameters and Its Application in Slope Earthquake Damage Prediction. *Chin. J. Geophys.* **1999**, *S1*, 101–107.
25. Grant, A.; Wartman, J.; Abou-Jaoude, G. Multimodal method for coseismic landslide hazard assessment. *Eng. Geol.* **2016**, *212*, 146–160. [CrossRef]
26. Wang, Y.; Zhang, M.-S.; Xue, Q.; Wu, S.-D. Risk-based evaluation on geological environment carrying capacity of mountain city—A case study in Suide County, Shaanxi Province, China. *J. Mt. Sci.* **2018**, *15*, 2730–2740. [CrossRef]
27. Sun, D.; Chen, Y.; Li, X.; Huang, C.; Su, H.; Chen, R. Control and Application of Terrain Curvature on Dynamic Disasters: A Case Study of Coal and Gas Outbursts in the Pingdingshan Mining Area, China. *Adv. Civ. Eng.* **2021**, *2021*, 1–6. [CrossRef]
28. Ye, Q.; Yu, S.; Liu, J.; Zhao, Q.; Zhao, Z. Aboveground biomass estimation of black locust planted forests with aspect variable using machine learning regression algorithms. *Ecol. Indic.* **2021**, *129*, 107948. [CrossRef]
29. Batar, A.; Watanabe, T. Landslide Susceptibility Mapping and Assessment Using Geospatial Platforms and Weights of Evidence (WoE) Method in the Indian Himalayan Region: Recent Developments, Gaps, and Future Directions. *ISPRS Int. J. Geo-Inf.* **2021**, *10*, 114. [CrossRef]
30. Dai, K.; Chen, C.; Shi, X.; Wu, M.; Feng, W.; Xu, Q.; Liang, R.; Zhuo, G.; Li, Z. Dynamic landslides susceptibility evaluation in Baihetan Dam area during extensive impoundment by integrating geological model and InSAR observations. *Int. J. Appl. Earth Obs. Geoinf.* **2023**, *116*, 103157. [CrossRef]
31. Meinhardt, M.; Fink, M.; Tünschel, H. Landslide susceptibility analysis in central Vietnam based on an incomplete landslide inventory: Comparison of a new method to calculate weighting factors by means of bivariate statistics. *Geomorphology* **2015**, *234*, 80–97. [CrossRef]
32. Manzo, G.; Tofani, V.; Segoni, S.; Battistini, A.; Catani, F. GIS techniques for regional-scale landslide susceptibility assessment: The Sicily (Italy) case study. *Int. J. Geogr. Inf. Sci.* **2013**, *27*, 1433–1452. [CrossRef]
33. Chen, W.; Xie, X.; Wang, J.; Pradhan, B.; Hong, H.; Bui, D.T.; Duan, Z.; Ma, J. A comparative study of logistic model tree, random forest, and classification and regression tree models for spatial prediction of landslide susceptibility. *Catena* **2017**, *151*, 147–160. [CrossRef]
34. Sharma, L.P.; Patel, N.; Debnath, P.; Ghose, M.K. Assessing landslide vulnerability from soil characteristics—A GIS-based analysis. *Arab. J. Geosci.* **2011**, *5*, 789–796. [CrossRef]
35. Zope, P.E.; Eldho, T.I.; Jothiprakash, V. Impacts of land use–land cover change and urbanization on flooding: A case study of Oshiwara River Basin in Mumbai, India. *Catena* **2016**, *145*, 142–154. [CrossRef]
36. Zhang, X.; Wu, Y.; Zhai, E.; Ye, P. Coupling analysis of the heat-water dynamics and frozen depth in a seasonally frozen zone. *J. Hydrol.* **2020**, *593*, 125603. [CrossRef]
37. Ye, F.; Sun, J.; Wang, Y.; Nedjah, N.; Bu, W. A novel method for the performance evaluation of institutionalized collaborative innovation using an improved G1-CRITIC comprehensive evaluation model. *J. Innov. Knowl.* **2023**, *8*, 100289. [CrossRef]
38. Behera, S.; Panigrahi, M.K. Gold prospectivity mapping and exploration targeting in Hutti-Maski schist belt, India: Synergistic application of Weights-of-Evidence (WOE), Fuzzy Logic (FL) and hybrid (WOE-FL) models. *J. Geochem. Explor.* **2022**, *235*, 106963. [CrossRef]
39. Wu, Z.; Lv, H.; Meng, Y.; Guan, X.; Zang, Y. The determination of flood damage curve in areas lacking disaster data based on the optimization principle of variation coefficient and beta distribution. *Sci. Total Environ.* **2021**, *750*, 142277. [CrossRef] [PubMed]
40. Puth, M.-T.; Neuhäuser, M.; Ruxton, G.D. Effective use of Spearman's and Kendall's correlation coefficients for association between two measured traits. *Anim. Behav.* **2015**, *102*, 77–84. [CrossRef]
41. Martens, F.K.; Tonk, E.C.; Kers, J.G.; Janssens, A.C.J. Small improvement in the area under the receiver operating characteristic curve indicated small changes in predicted risks. *J. Clin. Epidemiol.* **2016**, *79*, 159–164. [CrossRef]

Disclaimer/Publisher's Note: The statements, opinions and data contained in all publications are solely those of the individual author(s) and contributor(s) and not of MDPI and/or the editor(s). MDPI and/or the editor(s) disclaim responsibility for any injury to people or property resulting from any ideas, methods, instructions or products referred to in the content.